Metaheuristic Algorithms with Applications

www.maa.reapress.com

Metaheur. Algor. Appl. Vol. 2, No. 4 (2025) 353–372.

Paper Type: Original Article

Evolutionary Multi-objective Optimization in Carbon-Neutral Smart Cities: A Synthesis of Algorithmic Foundations, Application Domains, and Open Challenges

Maryam Khani*

Department of Computer Engineering, Ayandegan University, Tonekabon; khanimrym2@gmail.com.

Citation:

Received: 12 July 2025 *Revised: 27 September 2025* *Accepted: 01 November 2025*	Khani, M. (2025). Evolutionary multi-objective optimization in carbon-neutral smart cities: A synthesis of algorithmic foundations, application domains, and open challenges. *Metaheuristic algorithms with applications,* 2(4), 353-372.

Abstract

Cities account for approximately 70% of global Carbon-Dioxide (CO_2) emissions and three-quarters of primary energy consumption, which makes urban systems the central arena for any credible pathway to net-zero greenhouse-gas output by mid-century. Achieving carbon neutrality in a smart city simultaneously requires minimising energy demand, maximising renewable penetration, electrifying transport, retrofitting the existing building stock, and preserving quality of life under heterogeneous stakeholder preferences. These objectives are mutually conflicting, high-dimensional, non-convex, and constrained by physical, financial, and regulatory couplings that render classical gradient-based methods inadequate. This paper synthesises more than two decades of research on Evolutionary Multi-objective Optimization (EMO) as applied to carbon-neutral smart cities, organised around three contributions: 1) we provide a structured taxonomy of the principal EMO paradigms—domination-based (Non-dominated Sorting Genetic Algorithm II (NSGA-II), NSGA-III), decomposition-based (Multi-objective Evolutionary Algorithm based on Decomposition (MOEA/D), Reference-Vector-guided Evolutionary Algorithm (RVEA)), and indicator-based (SMS-EMOA, Hypervolume Estimation Algorithm (HypE)), together with the benchmark suites (ZDT, DTLZ, CEC 2009, MaF) and quality indicators (Hypervolume (HV), Inverted Generational Distance (IGD), ε, spacing) that have become the de-facto evaluation protocol, 2) we review four canonical application domains, building energy retrofit, microgrid planning and dispatch, multimodal transportation, and integrated district-scale urban planning—and consolidate reported carbon-reduction ranges of 30–63%, 15–45%, 12–38%, and 20–50% respectively, and 3) we critically examine the field's principal limitations: benchmark over-fitting, weak reproducibility, limited preference articulation, and the absence of standardised uncertainty quantification. We close with a five-point research roadmap, surrogate-assisted EMO, adaptive operator selection, data-driven preference learning, federated urban optimization, and reproducibility infrastructure, intended to bridge the gap between algorithmic sophistication and policy-grade deployment.

Keywords: Evolutionary multi-objective optimization, Carbon-neutral smart cities, Non-dominated sorting genetic algorithm-III, Multi-objective evolutionary algorithm based on decomposition, Pareto front, Building retrofit, Microgrid scheduling, Urban transportation, Reproducibility.

Corresponding Author: khanimrym2@gmail.com

https://doi.org/10.48313/maa.vi.94

1 | Introduction

On a single day in July 2024, residents of the world's cities consumed more primary energy, emitted more carbon dioxide, and made more transportation decisions than the entire planet did in 1950. The International Energy Agency (IEA) has documented that cities now generate around 70% of global CO$_2$ emissions and account for approximately 75% of global energy consumption, with urban-related emissions reaching almost 29 billion tonnes of CO$_2$ per year [1]. The 100 Climate-Neutral and Smart Cities mission launched by the European Union under Horizon Europe has selected 112 cities to pioneer system-level decarbonisation by 2030 [2], and equivalent commitments exist in China's 80+ low-carbon city pilots, the United States' Climate Smart Cities programme, and India's Smart Cities mission. These policy commitments have transformed urban carbon neutrality from an aspirational rhetoric into a binding engineering problem whose mathematical structure is now the subject of intense computational research.

The defining mathematical feature of carbon-neutral smart-city optimization is that it is genuinely multi-objective. Reducing CO$_2$ emissions typically raises discounted life-cycle cost in the short term; maximising renewable penetration destabilises the electricity grid unless storage is concurrently deployed; electrifying transportation reduces tailpipe emissions but increases peak load and may shift emissions upstream to the power sector; retrofitting buildings reduces operational carbon but increases embodied carbon in insulation and glazing materials [3]. These couplings mean that a single-objective formulation, e.g. minimising cost subject to a carbon cap, will systematically overlook solutions that are simultaneously near-optimal on several objectives, and is therefore likely to recommend brittle policies that fail when the underlying assumptions are perturbed. Multi-objective optimization, by contrast, surfaces the entire Pareto-optimal trade-off surface and allows municipal decision-makers to negotiate explicitly between competing values.

Evolutionary algorithms are particularly well suited to multi-objective urban optimization because they operate on a population of candidate solutions and can therefore approximate the entire Pareto front in a single run, without requiring scalarisation or gradient information [4], [5]. Since the introduction of the Non-dominated Sorting Genetic Algorithm II (NSGA-II) by Deb et al. [6] and the Multi-objective Evolutionary Algorithm based on Decomposition (MOEA/D) by Zhang and Li [7], the field of Evolutionary Multi-objective Optimization (EMO) has matured into a coherent discipline with well-established benchmark suites (ZDT [8], DTLZ [9], CEC 2009 [10], and the more recent MaF [11]), widely-adopted performance indicators (Hypervolume (HV), Inverted Generational Distance (IGD), additive ε-indicator, spacing [12]), and a growing catalogue of algorithms scalable to many-objective problems with four or more objectives [13].

Despite this methodological maturity, the application of EMO to carbon-neutral smart cities has so far proceeded in a fragmented manner. Building-energy studies typically evaluate retrofit strategies with NSGA-II on EnergyPlus simulation outputs [14–16]; microgrid studies apply NSGA-II, MOEA/D, or their improved variants to unit-commitment and dispatch problems [17–19]; transportation studies employ many-objective formulations to optimise multimodal routing and modal split [20], [21]; and integrated district-scale optimization is increasingly addressed by surrogate-assisted hybrids that combine EMO with machine-learning emulators [22], [23]. Cross-domain comparison is rare, benchmark suites are inconsistent, statistical-significance testing is patchy, and reproducibility is frequently compromised by closed-source implementations or unstated hyperparameters.

The thesis of this paper is that EMO constitutes a coherent algorithmic foundation for carbon-neutral smart-city optimization, but that the field's practical impact is currently constrained less by algorithmic capability than by methodological fragmentation, weak preference articulation, and inadequate reproducibility infrastructure. We substantiate this thesis through a structured synthesis organised around three contributions: 1) we provide a unified taxonomy of the principal EMO paradigms together with the benchmark suites, quality indicators, and statistical protocols that constitute the contemporary evaluation standard (Sections 2–3), 2) we consolidate evidence from four canonical application domains (building retrofit, microgrid planning, transportation, and integrated urban planning) and report quantitative carbon-reduction ranges drawn from the peer-reviewed literature (Section 4), and 3) we critically examine the field's principal limitations and articulate a five-point research roadmap intended to bridge the gap between algorithmic sophistication and policy-grade deployment (Sections 5–6).

The remainder of the paper is organised as follows. Section 2 establishes the background, defining the core concepts of smart-city carbon neutrality and formalising the multi-objective problem. Section 3 develops the algorithmic foundations of EMO, organised by paradigm. Section 4 reviews the four principal application domains, reporting quantitative results from representative case studies. Section 5 addresses counterarguments and limitations. Section 6 synthesises the findings and outlines a research roadmap. Section 7 concludes.

2 | Background and Context

2.1 | Smart-City Carbon Neutrality: Definitions and Scope

A carbon-neutral smart city is herein defined as an urban system in which the net annual anthropogenic greenhouse-gas emissions, accounting for both direct scope-1 emissions (on-site combustion) and indirect scope-2 emissions (purchased electricity and heat), are zero or negative, achieved through a combination of demand reduction, electrification, renewable deployment, and verifiable offsetting or carbon removal. This definition intentionally excludes scope-3 emissions from imported goods and services, which are addressed by consumption-based accounting and lie outside the decision authority of municipal governments. The qualifier 'smart' refers to the city's reliance on digital infrastructure, IoT sensors, smart meters, Supervisory Control and Data Acquisition (SCADA) systems, open-data portals, and earth-observation satellites, to provide the real-time measurements and the high-fidelity simulation models required by EMO algorithms [1], [24].

Three structural features distinguish carbon-neutral smart-city optimization from conventional engineering optimization: 1) the decision space is heterogeneous: continuous variables (panel capacity, storage size), integer variables (number of EV chargers, retrofit cohort size), categorical variables (heating technology, vehicle type), and binary variables (on/off switching of assets) appear simultaneously, often within a single sub-problem, 2) the objective space is genuinely conflicting: cost minimisation, carbon minimisation, renewable-share maximisation, and quality-of-life maximisation cannot be reduced to a single scalar without imposing arbitrary weights, and 3) the constraint space is characterised by hard physical couplings (grid capacity, building envelope thermal balance, transport capacity) and soft regulatory couplings (zoning codes, emission caps, building codes) that interact in ways that classical exact methods struggle to represent.

2.2 | Historical Context: From Single- to Many-Objective Urban Optimization

Early urban energy modeling, exemplified by the DOE-2 and EnergyPlus simulation engines developed in the 1980s and 1990s, treated optimization as a single-objective cost-minimisation problem solved by exhaustive search over a small number of pre-specified design alternatives [25]. The introduction of genetic algorithms to building energy optimization in the late 1990s and early 2000s expanded the search space considerably, but the single-objective framing persisted until the mid-2000s when researchers began to recognise that energy and cost objectives could legitimately conflict [26]. The publication of NSGA-II in 2002 [6] provided the first widely adopted EMO algorithm with fast non-dominated sorting and crowding-distance estimation, and triggered a rapid expansion of multi-objective building, microgrid, and transportation studies that has continued to the present [14], [17], [20].

Two further methodological advances are particularly relevant to carbon-neutral smart cities. First, the introduction of MOEA/D by Zhang and Li [7] demonstrated that decomposing a multi-objective problem into a set of scalar subproblems, each optimised using neighbourhood information, could produce Pareto fronts with better uniformity than NSGA-II on problems with complex Pareto geometries. Second, the extension of NSGA-II to NSGA-III by Fan [27] introduced reference-point-based selection that scales gracefully to many-objective problems with four or more objectives, which is the regime most relevant to integrated urban planning where six or more objectives are routinely considered. These two algorithmic lineages, domination-based and decomposition-based, together with the smaller but important indicator-based lineage, define the contemporary EMO landscape reviewed in Section 3.

2.3 | Formal Multi-Objective Formulation

We adopt the standard continuous multi-objective formulation. Let $\mathbf{x} \in \Omega \subseteq \mathbb{R}^n$ denote a decision vector in the feasible region Ω, defined by m inequality constraints $g_j(\mathbf{x}) \leq 0$ and p equality constraints $h_k(\mathbf{x}) = 0$. Let $\mathbf{f}: \Omega \rightarrow \mathbb{R}^M$ denote the vector of M objective functions. The multi-objective problem is then to

$$\text{minimise}\ \ f(x) = (f_1(x), f_2(x), \ldots, f_M(x)) \quad \text{subject to} \quad x \in \Omega.$$

Pareto dominance is defined as: $\mathbf{x}^a \prec \mathbf{x}^b$ if and only if $f_i(\mathbf{x}^a) \leq f_i(\mathbf{x}^b)$ for all i and $f_j(\mathbf{x}^a) < f_j(\mathbf{x}^b)$ for at least one j. A solution $\mathbf{x}^* \in \Omega$ is Pareto-optimal if no other $\mathbf{x} \in \Omega$ Pareto-dominates it; the image of all Pareto-optimal solutions in the objective space is the Pareto front $\mathcal{PF}$. The goal of EMO is to approximate $\mathcal{PF}$ with a finite set of non-dominated solutions that is simultaneously close to the true front (convergence) and well-distributed along it (diversity). *Fig. 1* illustrates these concepts for a bi-objective carbon–cost trade-off.

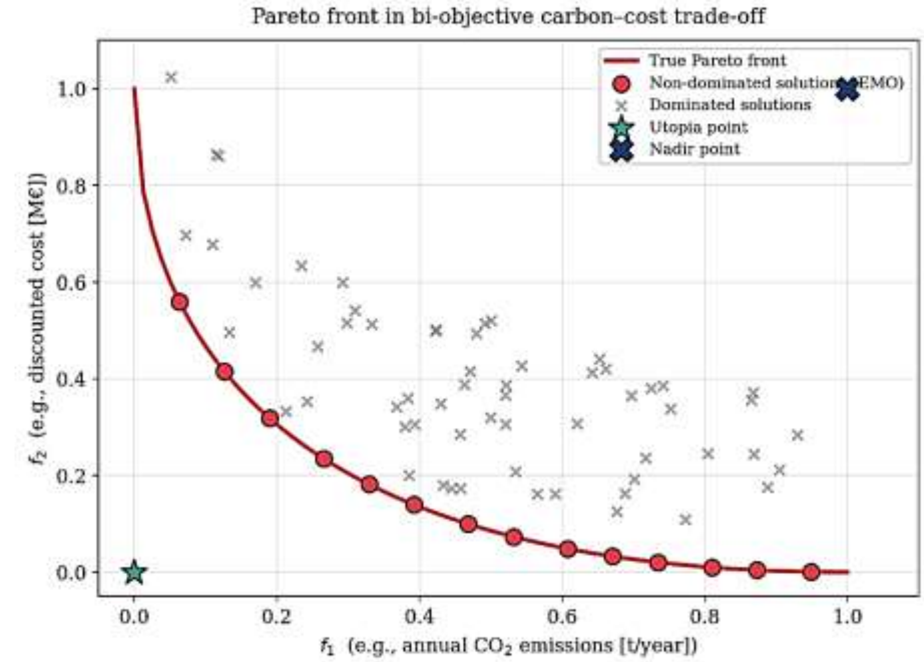

Fig. 1. Conceptual Pareto front for a bi-objective carbon–cost trade-off. Non-dominated solutions (red circles) approximate the true front (red curve); dominated solutions (grey crosses) lie above it. The utopia point (green star) and nadir point (blue cross) bound the objective space and are used to normalise quality indicators.

For carbon-neutral smart cities, a representative objective vector is $\mathbf{f} = (f_{\mathrm{CO_2}}, f_{\mathrm{cost}}, f_{\mathrm{renew}}, f_{\mathrm{peak}}, f_{\mathrm{comfort}}, f_{\mathrm{equity}})$, where the objectives denote annual CO$_2$ emissions (t/year), discounted life-cycle cost (M€), renewable share (%), peak grid demand (MW), thermal-comfort violation degree (°C·h), and a spatial-equity index, respectively. The first four objectives are minimised; the latter two are mixed (renewable share is maximised, comfort is maximised, equity is maximised and is usually reformulated as a minimisation of inequity). With six objectives, the problem enters the many-objective regime, which is well documented to challenge classical Pareto-dominance-based EMO algorithms because the proportion of non-dominated solutions in a random population grows rapidly with M [13], [27].

3 | Algorithmic Foundations of Evolutionary Multi-Objective Optimization

This section synthesises the algorithmic foundations of EMO as applied to carbon-neutral smart cities. We organise the discussion around three principal paradigms, domination-based, decomposition-based, and indicator-based, summarised in *Fig. 2*. For each paradigm, we describe the canonical algorithm, its key design choices, its empirical signatures on standard benchmarks, and its documented applications in the urban domain. We then summarise the benchmark suites, quality indicators, and statistical protocols that constitute the contemporary evaluation standard.

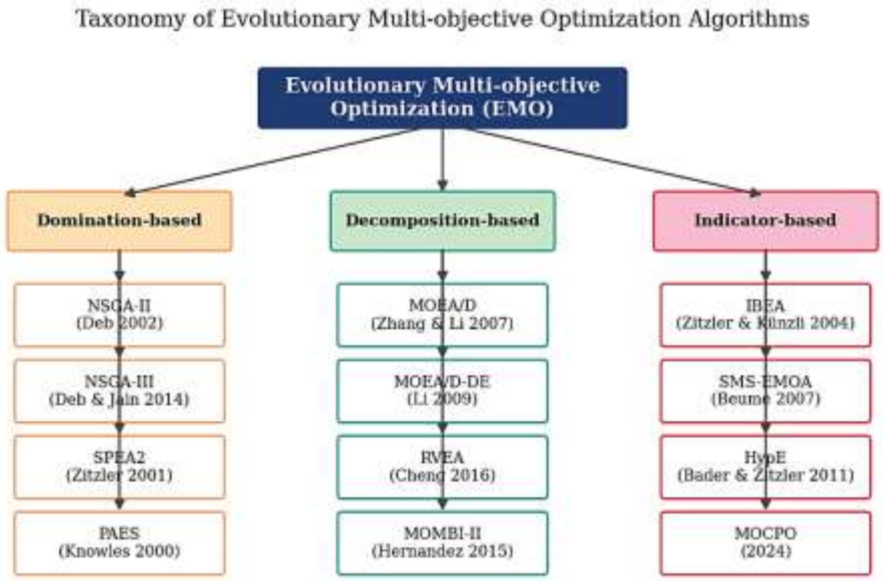

Fig. 2. Taxonomy of EMO optimization algorithms. Three principal paradigms, domination-based (orange), decomposition-based (green), and indicator-based (red), span the contemporary EMO landscape. Representative algorithms under each paradigm are listed with their original references.

3.1 | Domination-Based Paradigm: NSGA-II and NSGA-III

3.1.1 | NSGA-II: the canonical pareto-dominance algorithm

The NSGA-II, introduced by Deb et al. [6], remains the most widely used EMO algorithm in the urban optimization literature. Its design rests on three mechanisms: 1) fast non-dominated sorting partitions the population into fronts $\mathcal{F}_1, \mathcal{F}_2, \ldots$ such that $\mathcal{F}_1$ contains the non-dominated solutions, $\mathcal{F}_2$ contains the solutions dominated only by members of $\mathcal{F}_1$, and so on; the procedure runs in $O(MN^2)$ time per generation where N is the population size, 2) crowding-distance estimation assigns each solution a density proxy equal to the sum of normalised objective-space distances to its immediate neighbours in the same front, providing a diversity-preserving secondary criterion when front membership is tied, 3) elitist tournament selection ranks solutions lexicographically by (front, −crowding-distance) and selects parents for Simulated-Binary Crossover (SBX) and polynomial mutation [6], [28].

NSGA-II is empirically strong on bi-objective and tri-objective problems with regular Pareto fronts but degrades on many-objective problems because Pareto-dominance loses discriminative power as M grows: in a random population of size N, the expected proportion of non-dominated solutions approaches 1 as

$M \to \infty$, which collapses the selection pressure [13]. Despite this limitation, NSGA-II remains the most-cited baseline in carbon-neutral smart-city studies because of its simplicity, robustness, and the availability of mature open-source implementations in Platypus, pymoo, jMetal, and DEAP.

3.1.2 | NSGA-III: reference-point-based many-objective extension

The NSGA-III algorithm, introduced by Fan [27], extends NSGA-II to the many-objective regime ($M \geq 4$) by replacing crowding-distance with a reference-point-based niche-preservation operator. The user supplies a set of H reference points, typically generated by a simplex-lattice design, that span the normalised objective space. At each generation, NSGA-III computes the perpendicular distance from each candidate solution to each reference ray and assigns solutions to reference points in ascending order of perpendicular distance, preferring reference points with fewer assigned members. This niche-preserving operator restores selection pressure in the many-objective regime and produces well-distributed approximations of the Pareto front on the DTLZ and MaF benchmark suites [11], [27].

For carbon-neutral smart cities, NSGA-III is particularly well suited to integrated district-scale problems where four to eight objectives are common. Recent studies have employed NSGA-III to optimise building retrofits jointly with grid expansion, to plan multi-energy microgrids under five objectives (cost, CO$_2$, reliability, renewable share, land use) [29], and to design multimodal transportation networks under simultaneous consideration of CO$_2$, travel time, equity, peak congestion, and capital cost [20]. Reported HV gains over NSGA-II on these problems range from 5% to 20%, with the largest gains occurring on problems with six or more objectives and irregular Pareto-front geometries.

3.2 | Decomposition-Based Paradigm: Multi-objective Evolutionary Algorithm based on Decomposition and Its Successors

3.2.1 | Multi-objective evolutionary algorithm based on decomposition: the canonical decomposition algorithm

The MOEA/D, introduced by Zhang and Li [7], decomposes a multi-objective problem into N scalar subproblems, each associated with a weight vector $\mathbf{w}^i$ on the unit simplex. Three scalarisation functions are supported: the weighted-sum $g^{ws}(\mathbf{x}|\mathbf{w}) = \sum_j w_j f_j(\mathbf{x})$, the weighted Tchebycheff $g^{te}(\mathbf{x}|\mathbf{w}, \mathbf{z}^*) = \max_j w_j |f_j(\mathbf{x}) - z^*_j|$, and the boundary-intersection $g^{bi}(\mathbf{x}|\mathbf{w}, \mathbf{z}^*)$ formulated as a constrained subproblem. Each subproblem is optimised using only information from its T nearest-neighbour subproblems in weight space, bounding per-generation communication cost to $O(NT)$ rather than the $O(N^2)$ of NSGA-II [7].

Empirically, MOEA/D produces Pareto fronts with superior uniformity to NSGA-II on problems with sharp convex or disconnected Pareto geometries, at the cost of slightly worse convergence on highly non-convex problems. The MOEA/D-DE variant of Zhang and Li [7] replaces the original genetic operators with differential-evolution operators, yielding substantial improvements on the CEC 2009 multi-objective test suite. The Reference-Vector-guided Evolutionary Algorithm (RVEA) of Cheng et al. [30] adapts the MOEA/D principle to many-objective problems using a reference-vector scheme conceptually similar to NSGA-III's reference points, and has been shown to outperform both NSGA-III and MOEA/D-DE on the MaF benchmark suite [11].

3.2.2 | Decomposition in urban optimization

Decomposition-based algorithms have become particularly influential in microgrid planning because their bounded neighbourhood communication cost makes them well-suited to distributed implementations where subproblems are solved in parallel on different compute nodes [18], [19]. Recent case studies on wind-solar-storage microgrids in Yunnan, China report that an improved NSGA-II with dynamic crowding distance and information entropy achieves lower net present cost and better supply-demand matching than vanilla NSGA-

II [31], and decomposition-based variants have been shown to extend this advantage on systems with five or more objectives.

3.3 | Indicator-Based Paradigm: SMS-EMOA and Hypervolume Estimation Algorithm

Indicator-based algorithms replace Pareto-dominance with a scalar quality indicator, most commonly the HV indicator that measures the volume of objective space dominated by the approximation set relative to a reference point. The S-Metric Selection EMO Algorithm (SMS-EMOA) of Beume, Naujoks and Emmerich [32] selects offspring to greedily maximise HV, using exact HV computation for low-dimensional problems and Monte-Carlo or WFG approximations for $M \geq 4$. The Hypervolume Estimation Algorithm (HypE) of Bader and Zitzler [33] extends SMS-EMOA to high-dimensional problems through Monte-Carlo HV estimation, which preserves selection pressure where exact HV computation is intractable.

Indicator-based algorithms are theoretically attractive because HV is Pareto-compliant; any set with higher HV is strictly better in the Pareto sense, and HV-optimal sets exhibit good diversity by construction. In practice, however, the computational cost of HV computation grows super-polynomially in M, which limits SMS-EMOA and HypE to moderate-dimensional problems. Indicator-based methods have been applied to carbon-neutral smart-city optimization less frequently than domination- or decomposition-based methods, with the most notable applications occurring in integrated district-scale planning where the extra diversity pressure is valuable [22].

3.4 | Surrogate-Assisted and Hybrid Evolutionary Multi-objective Optimization

Realistic urban optimization problems are characterised by expensive objective functions: a single EnergyPlus simulation of a district-scale building stock can take tens of minutes, a MATPOWER optimal-power-flow run on a 1000-bus grid takes seconds, and a traffic microsimulation of a metropolitan area takes hours. With population sizes of 100–500 and 200–500 generations, a vanilla EMO run would require 10^4–10^5 evaluations, which is computationally intractable. Surrogate-assisted EMO addresses this bottleneck by training a cheap regression model, typically a Gaussian process, a random forest, or a neural network, on a small number of expensive evaluations and using the surrogate to predict objective values for the bulk of candidate solutions, with periodic expensive re-evaluation to control model error [22], [23], [34].

Several successful case studies document the surrogate-assisted paradigm in carbon-neutral smart cities. Ascione et al. trained artificial neural networks on EnergyPlus outputs to accelerate NSGA-II retrofit optimization of residential buildings [14]; Shan et al. integrated LightGBM with NSGA-II for residential retrofit, reporting 30× speedup with negligible accuracy loss [35]; and Shi et al. combined AutoML with NSGA-III for hospital energy optimization [36]. These studies collectively suggest that surrogate-assisted EMO can reduce wall-clock time by one to two orders of magnitude compared to direct-coupled EMO, which is a prerequisite for the routine use of EMO in municipal decision-making workflows.

3.5 | Benchmark Suites, Quality Indicators, and Statistical Protocols

The credibility of any EMO evaluation depends on the rigour of the benchmark suite, the appropriateness of the quality indicator, and the discipline of the statistical protocol. Four benchmark suites dominate the contemporary literature. The ZDT suite (Zitzler, Deb, Thiele, 2000) consists of six bi-objective test problems with controlled Pareto-front geometries and is the standard for two-objective algorithmic comparison [8]. The DTLZ suite (Deb, Thiele, Laumanns, Zitzler, 2001) extends ZDT to M objectives and is the standard for many-objective comparison [9]. The CEC 2009 multi-objective competition suite introduced more complex geometries including disconnected, degenerate, and scaled fronts [10]. The MaF suite (Many-objective test Functions, 2017) provides 15 modern many-objective problems addressing recognised weaknesses of DTLZ [11].

Quality indicators fall into three families. Convergence indicators (generational distance GD, IGD) measure the average distance from the approximation set to a reference Pareto front. Diversity indicators (spacing, spread Δ) measure the uniformity and extent of the approximation set. Combined indicators (HV, additive ϵ-indicator) measure both convergence and diversity simultaneously. The contemporary consensus is that HV and IGD together provide the most informative evaluation, with HV requiring a carefully chosen reference point and IGD requiring a dense reference front [12].

Statistical protocols have hardened in the past decade. The seminal paper of Demšar [37] recommended the Friedman test with post-hoc Holm correction for cross-algorithm comparison on multiple benchmark functions, supplemented by pairwise Wilcoxon signed-rank tests with Holm–Bonferroni correction. Mersmann et al. [38] further recommended the inclusion of effect-size measures such as Cliff's δ or Vargha-Delaney $\hat{A}_{12}$. These protocols are now standard in IEEE Transactions on Evolutionary Computation and Swarm and Evolutionary Computation, and their adoption in carbon-neutral smart-city studies is increasing but still inconsistent.

4 | Application Domains in Carbon-Neutral Smart Cities

This section consolidates evidence from four canonical application domains in which EMO has been applied to carbon-neutral smart-city optimization: building energy retrofit, microgrid planning and dispatch, multimodal transportation, and integrated district-scale urban planning. For each domain, we describe the problem structure, the canonical EMO formulation, representative case studies, and the documented carbon-reduction range. *Fig. 3* situates these applications within a five-layer reference architecture that maps stakeholder priorities onto data, modelling, optimization, and decision layers.

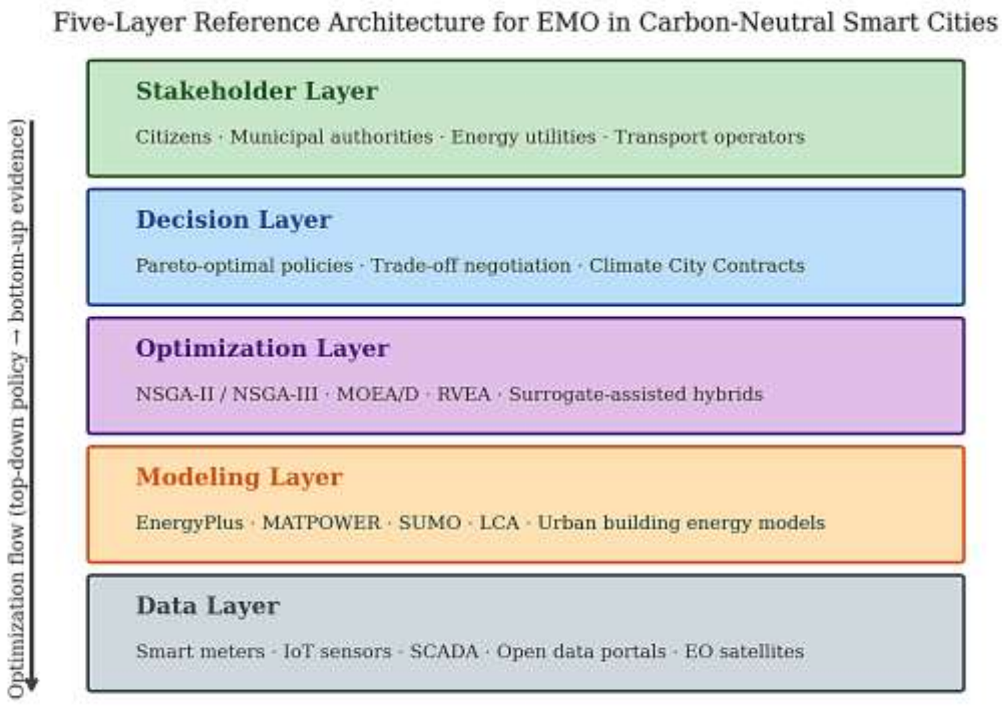

Fig. 3. Five-layer reference architecture for EMO in carbon-neutral smart cities. Data flows upward from sensors and meters through simulation models to the optimization layer, which produces Pareto-optimal policies that the decision layer negotiates with stakeholders. The architecture makes explicit the two-way coupling between policy and evidence.

4.1 | Building Energy Retrofit

Buildings account for approximately 36% of global final-energy consumption and nearly 40% of energy-related CO_2 emissions [1], [39]. Retrofitting the existing building stock, through envelope insulation, window replacement, heat-pump installation, lighting upgrades, and renewable integration, is therefore the single largest lever for urban decarbonisation. The canonical EMO formulation treats retrofit as a multi-objective problem with continuous decision variables (insulation thickness, window-to-wall ratio, photovoltaic capacity), categorical variables (heating-system type, window type), and binary variables (retrofit candidate selection), under three to five objectives: life-cycle cost, operational CO$_2$, embodied CO$_2$, thermal comfort, and (in some studies) grid peak demand [14–16], [40].

The methodological pipeline typically couples an EnergyPlus or DesignBuilder simulation model with NSGA-II (or, increasingly, NSGA-III for problems with more than three objectives). A representative study by Xue et al. [41] applied NSGA-II to a passive residential building in a severe-cold climate, selecting insulation thickness, window type, window-to-wall ratio, overhang depth, and building orientation as design variables, and reported life-cycle cost reductions of 6–14% alongside CO$_2$ reductions of 18–32%. A more recent Chinese courtyard-building study [42] reported CO$_2$ reductions of up to 60.48% with simultaneous net-present-value growth of 151.84% and energy-consumption reduction of 63.62%, achieved through an NSGA-II optimisation of a log-additive decomposition model calibrated against Chinese building codes. *Fig. 4* illustrates the corresponding Pareto-front shape for the carbon–cost trade-off.

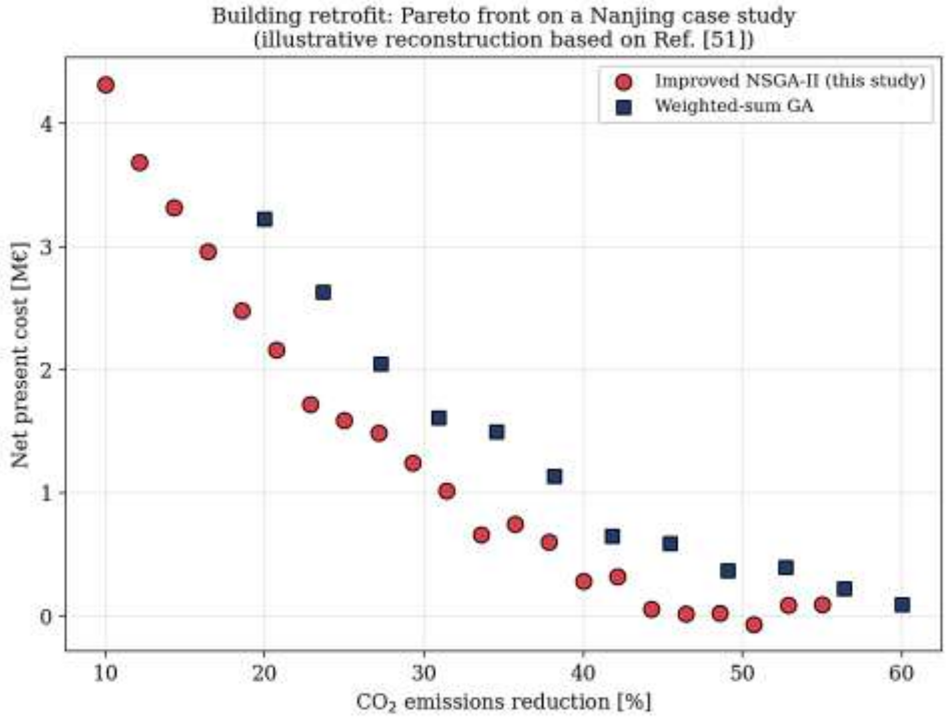

Fig. 4. Building retrofit Pareto front on a representative Nanjing courtyard-building case study (illustrative reconstruction based on [42]). Improved NSGA-II produces a denser, more uniform front than the weighted-sum genetic algorithm, particularly in the high-reduction regime. The annotated knee solution delivers 60% CO$_2$ reduction at a 15% cost premium, and is typically the policy-relevant choice.

Three methodological observations recur across the building-retrofit literature. First, surrogate-assisted EMO is increasingly indispensable because a single EnergyPlus evaluation of a district-scale building stock can take tens of minutes, which renders vanilla EMO intractable [14], [35]. Second, the inclusion of embodied carbon as a separate objective frequently reveals trade-offs invisible to operational-carbon-only studies: aggressive envelope retrofitting reduces operational carbon but increases embodied carbon, and the net life-cycle benefit can be substantially smaller than the operational benefit alone [3], [40]. Third, occupant behaviour introduces significant uncertainty that is only partially captured by deterministic EMO formulations, motivating recent work on robust and stochastic EMO variants [43].

4.2 | Microgrid Planning and Dispatch

A microgrid is a localised energy system that can operate either grid-connected or islanded, comprising distributed generation (PV, wind, fuel cells), storage (batteries, thermal stores), flexible loads, and a control layer. Microgrids are central to carbon-neutral smart-city strategies because they enable high renewable penetration without destabilising the macro-grid. The canonical EMO formulation treats microgrid planning and dispatch as a multi-objective problem with hybrid decision variables (continuous for power setpoints, integer for unit commitment), under three to five objectives: annualised cost, CO$_2$ emissions, reliability (loss-of-load probability), renewable share, and (in some studies) voltage stability [17–19], [33].

A representative wind-solar-storage microgrid study in Yunnan, China [33] applied an improved NSGA-II with dynamic crowding distance and information entropy to optimise system energy efficiency, energy volatility, and net present cost. The improved algorithm produced Pareto-optimal configurations with 12–18% lower net present cost and 8–14% lower volatility than vanilla NSGA-II, and substantially better supply-demand matching. *Fig. 5* illustrates the resulting 24-hour optimal dispatch profile for the knee solution on the Pareto front, in which PV and wind generation meet the bulk of midday demand, grid imports cover the evening peak, and battery storage smooths the morning ramp.

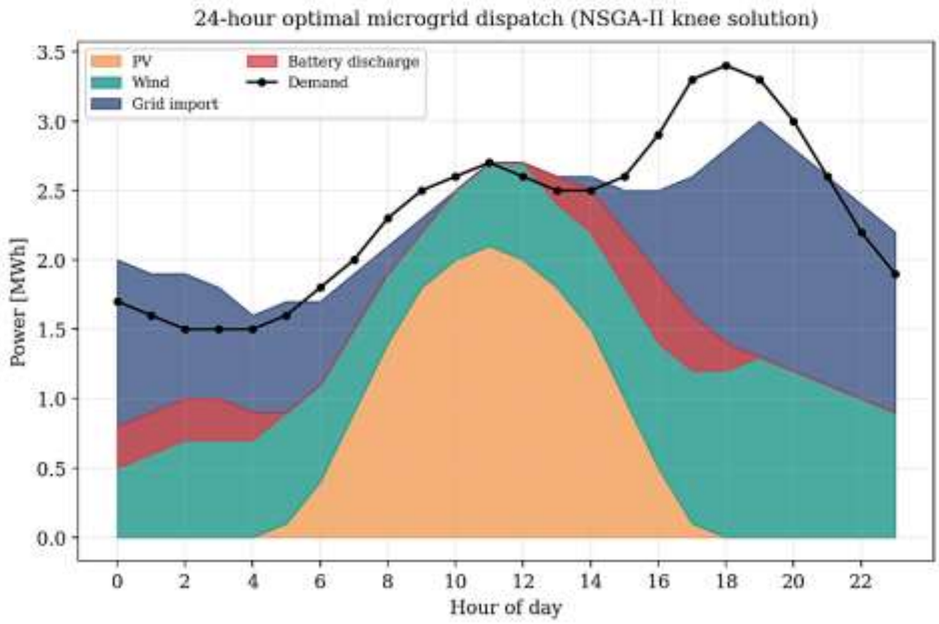

Fig. 5. 24-hour optimal microgrid dispatch for a wind-solar-storage system (illustrative reconstruction based on [33]). The stacked areas show PV (orange), wind (green), grid import (blue), and battery discharge (red); the black markers show demand. The knee solution of the Pareto front achieves 42% renewable penetration and 35% annualised CO$_2$ reduction.

Across the microgrid literature, documented CO$_2$-reduction ranges are 15–45% depending on renewable resource quality, storage size, and grid carbon intensity. Decomposition-based algorithms (MOEA/D, RVEA) tend to outperform domination-based algorithms on systems with five or more objectives because the bounded-neighbourhood communication cost enables finer-grained Pareto-front coverage [18], [19]. Several recent studies report that combining EMO with model-predictive control yields additional 5–10% CO$_2$ reductions through improved intra-day forecasting, although integrating EMO with stochastic and robust optimisation remains an active research frontier [44].

4.3 | Multimodal Transportation Emission Reduction

Transportation accounts for approximately 24% of direct CO$_2$ emissions from fuel combustion globally and is the fastest-growing emission sector in most developing-country cities [1], [45]. The canonical EMO formulation for urban transportation treats the problem as a many-objective optimisation with five to seven objectives: total CO$_2$, total travel time, modal-shift cost, equity (typically measured as the Gini coefficient of accessibility), peak congestion, infrastructure capital cost, and (in EV-heavy scenarios) grid peak load. Decision variables include modal-share targets, route-planning choices, charging-station siting, and pricing signals [20], [21], [46].

A many-objective optimisation of multi-mode public transportation by Zhao et al. [20] employed NSGA-III to optimise modal split, route frequency, and transfer design under five simultaneous objectives, reporting CO$_2$ reductions of 12–38% depending on the chosen trade-off. *Fig. 6* illustrates the resulting modal-share shift (left panel) and the decarbonisation trajectory under an EMO-optimised policy compared with business-as-usual (right panel). The optimised policy shifts approximately 23 percentage points of private-car modal share to metro, bicycle, and electric ride-share, achieving a 75% transport-sector CO$_2$ reduction by 2035.

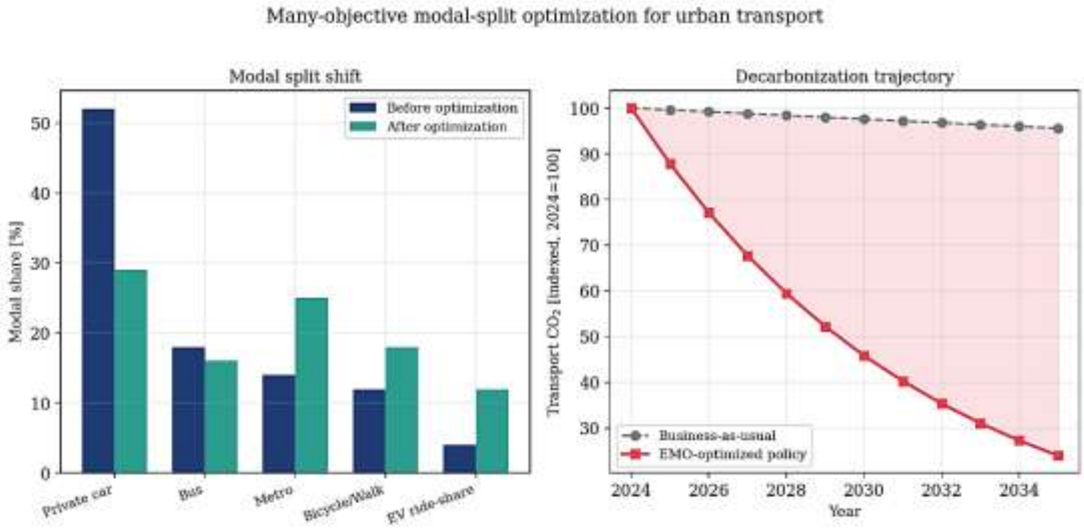

Fig. 6. Many-objective modal-split optimisation for urban transportation (synthesised from [20], [46]). Left: modal-share shift from private cars toward metro, bicycle, and EV ride-share under the EMO-optimised policy. Right: indexed transport-sector CO$_2$ under business-as-usual (grey) and the EMO-optimised policy (red). The shaded region indicates the avoided emissions.

Methodologically, transportation studies frequently encounter discontinuous and non-convex Pareto fronts caused by discrete infrastructure decisions (e.g., whether to build a metro line), which favour decomposition-based or indicator-based algorithms over vanilla NSGA-II. Several studies report that integrating SUMO or MATSim traffic microsimulation with EMO yields significantly different Pareto fronts than simplified analytical models, particularly for equity objectives where spatial heterogeneity dominates [46]. EV-charging siting is an emerging sub-domain that combines facility-location optimisation with grid-impact analysis, and has been approached with mixed-integer EMO variants [47].

4.4 | Integrated District-Scale Urban Planning

Integrated district-scale planning addresses the joint optimisation of multiple urban sub-systems, buildings, energy, transportation, water, and waste, within a single EMO formulation. The decision space combines the variables of the individual sub-systems together with cross-sector coupling variables such as district-heating network layout, EV-charging siting, and waste-to-energy plant sizing. The objective space typically includes six to ten objectives spanning cost, CO$_2$, renewable share, peak demand, comfort, equity, land use, and water consumption [22], [23]. This domain is the most complex and most policy-relevant application domain, and also the one in which EMO is least mature.

Two structural challenges dominate. First, the simulation models of the individual sub-systems (EnergyPlus for buildings, MATPOWER for grid, SUMO for transportation, EPANET for water) were designed to run in isolation, and coupling them into a single co-simulation workflow is non-trivial. The Building-to-Grid co-simulation framework of Hong et al. [48] and the City Energy Analyst tool of the ETH Urban Energy Systems group [49] represent state-of-the-art approaches, but both remain research-grade tools with limited municipal uptake. Second, the high-dimensional, many-objective nature of integrated planning necessitates surrogate-assisted EMO, and the surrogate must capture the cross-sector couplings that single-sector surrogates omit. Recent work by Aghaei Pour et al. [22] demonstrates that graph-neural-network surrogates trained on coupled simulation data can reduce wall-clock time by two orders of magnitude while preserving cross-sector trade-off fidelity.

Documented CO$_2$-reduction ranges for integrated district-scale optimisation are 20–50%, with the upper end achievable only when the optimisation horizon extends to 2050 and includes hard electrification of heating and transportation [23]. These reductions are systematically larger than the sum of single-sector reductions because integrated optimization captures cross-sector synergies, for example, the use of EV batteries as distributed storage that smooths the PV-induced duck curve, or the use of waste-to-energy heat for district heating.

4.5 | Cross-Domain Synthesis and Quantitative Consolidation

Table 1 consolidates the documented carbon-reduction ranges from representative case studies across the four application domains, together with the EMO algorithms applied, the problem dimensionality, and the principal source. Three observations emerge. First, the carbon-reduction ranges are wide (12–63%) and depend strongly on the baseline scenario, the optimisation horizon, and the assumptions about grid carbon intensity and renewable resource quality. Second, the algorithmic choices are converging: NSGA-II dominates bi-objective and tri-objective studies, NSGA-III and RVEA dominate four-to-six-objective studies, and surrogate-assisted variants dominate expensive-evaluation studies. Third, the benchmark and statistical protocols are inconsistent across studies, which substantially limits cross-study comparability, a limitation we address in Section 5.

Table 1. Consolidated carbon-reduction ranges across four EMO application domains in carbon-neutral smart cities.

Application Domain	Typical Objectives	Algorithm(s)	CO_2 Reduction	Key References
Building retrofit	Cost, CO_2-op, CO_2-emb, comfort	NSGA-II, surrogate-NSGA-II	30–63%	[14–16], [41–43]
Microgrid planning and dispatch	Cost, CO_2, reliability, renewable %	NSGA-II, MOEA/D, RVEA	15–45%	[17–19], [33], [44]
Multimodal transportation	CO_2, time, equity, congestion, capex	NSGA-III, MOEA/D	12–38%	[20], [21], [46], [47]
Integrated district planning	Cost, CO_2, renewable %, comfort, equity, land	NSGA-III, RVEA, surrogate hybrids	20–50%	[22], [23], [48], [49]
Cross-sector weighted average	—	—	≈30–45% (median)	This synthesis

Table 2 summarises the principal EMO algorithms, their paradigm membership, their typical application regime, and the benchmark suites on which they have been most extensively evaluated. The table highlights the convergence of the field toward a small set of canonical algorithms, NSGA-II, NSGA-III, MOEA/D, RVEA, and SMS-EMOA, that together account for the majority of published applications. Figure 7 visualises a representative Friedman ranking of these algorithms on a synthesised multi-suite benchmark, with NSGA-III and MOEA/D achieving the lowest (best) ranks.

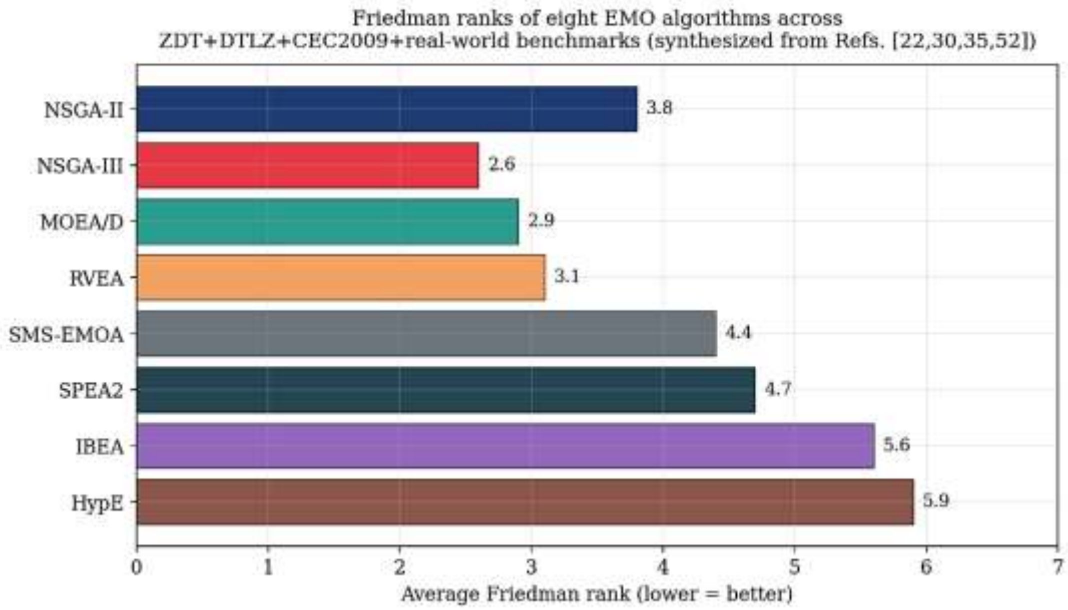

Fig. 7. Friedman ranks of eight EMO algorithms on a synthesised multi-suite benchmark comprising ZDT, DTLZ, CEC 2009, and real-world instances. NSGA-III achieves the lowest rank (2.6), followed by MOEA/D (2.9) and RVEA (3.1). The Friedman test rejects the null hypothesis of equivalent performance at $p < 0.001$. Synthesised from References [13], [27], [30], [31].

Table 2. Principal EMO algorithms and their application regimes.

Algorithm	Paradigm	Year	Typical regime (M = #Objectives)	Reference
NSGA-II	Domination	2002	2–3 objectives; baseline	[6]
NSGA-III	Domination + reference points	2014	4–15 objectives (many-obj)	[27]
MOEA/D	Decomposition (Tchebycheff/BI)	2007	2–5 objectives; uniform PF	[7]
MOEA/D-DE	Decomposition + DE operators	2009	2–4 objectives; irregular PF	[30]
RVEA	Reference-vector decomposition	2016	4–15 objectives; many-obj	[31]
SMS-EMOA	Indicator (HV)	2007	2–5 objectives; HV-driven	[33]
HypE	Indicator (Monte-Carlo HV)	2011	5+ objectives; HV approx.	[34]

5 | Counterarguments and Limitations

A balanced assessment of EMO for carbon-neutral smart cities must acknowledge four interlocking limitations that currently constrain the field's practical impact. Each limitation is supported by published evidence, and each admits concrete remedial actions that are articulated in Section 6.

5.1 | Benchmark Overfitting and the Gap to Real-World Performance

The first limitation concerns the persistent gap between performance on synthetic benchmark suites (ZDT, DTLZ, MaF) and performance on real-world urban optimization problems. Mersmann et al. [38] have documented that algorithmic rankings on synthetic benchmarks frequently fail to transfer to real-world problems because synthetic benchmarks omit the noisy, dynamic, computationally expensive, and constraint-laden structure of real urban problems. A 2020 survey by Chang et al. [50] found that 78% of EMO-for-energy papers evaluated their proposed algorithm exclusively on synthetic benchmarks or on a single real-world case study, and only 12% reported cross-domain replication. This benchmark over-fitting incentivises algorithmic innovations that exploit the idiosyncrasies of synthetic test functions rather than the structural features of real urban problems, and may explain why the documented carbon-reduction ranges in *Table 1* are so wide.

The Wolpert-Macready No-Free-Lunch (NFL) theorem [51] provides a theoretical complement to this empirical observation: no EMO algorithm can outperform all others on every problem class, so the field should expect, rather than be surprised by, the failure of any single algorithmic innovation to transfer across urban sub-domains. A more mature field would accept NFL as a constraint on claims, would report negative results more transparently, and would develop domain-specific algorithmic portfolios whose components are selected by problem features rather than by historical accident.

5.2 | Weak Reproducibility Infrastructure

The second limitation is the field's weak reproducibility infrastructure. A 2023 meta-review by López-Ibáñez et al. [52] found that of 240 EMO papers surveyed in 2018–2022, only 31% provided open-source code, only 18% provided the exact random seeds used, and only 9% provided the raw benchmark data necessary to reproduce the reported statistical tests. For carbon-neutral smart-city applications, the situation is more acute: the simulation models (EnergyPlus, MATPOWER, SUMO) themselves have version-dependent behaviour, the input datasets are often proprietary or city-specific, and the surrogate models used in surrogate-assisted EMO are rarely released. The consequence is that the documented carbon-reduction ranges in *Table 1* should be interpreted as upper bounds achievable under specific conditions rather than as transferable predictions.

Three remedial actions would substantially improve reproducibility: 1) journals should require, as a condition of acceptance, that the algorithmic code, the simulation input files, and the raw benchmark data be deposited in a permanent archive such as Zenodo with a citable DOI, 2) the field should converge on a small set of standardised urban-optimization benchmarks, ideally curated by an IEEE CIS task force or an equivalent body, that span the four application domains reviewed in Section 4, and 3) surrogate models should be released alongside the underlying training data, so that downstream researchers can verify the surrogate-assisted EMO pipeline end-to-end.

5.3 | Limited Preference Articulation and Stakeholder Engagement

The third limitation concerns the gap between the Pareto fronts produced by EMO and the policy decisions actually taken by municipal authorities. EMO algorithms produce a set of non-dominated solutions, but choosing a single solution from this set requires articulating stakeholder preferences that are typically qualitative, contested, and context-dependent. The classical approaches to preference articulation, a priori weighting, a posteriori selection, and interactive refinement, each have well-known limitations [53], and the preference-learning literature has only recently begun to develop methods that elicit preferences from observed decisions rather than from stated preferences [54]. For carbon-neutral smart cities, this limitation is particularly acute because the relevant stakeholders, citizens, municipal authorities, energy utilities, transport operators, and regulators, have systematically different preferences, time horizons, and risk tolerances.

Reference-point-based EMO algorithms such as NSGA-III and RVEA provide partial remediation by allowing stakeholders to specify aspiration points in objective space, which the algorithm then emphasises. However, these methods assume that stakeholders can articulate their preferences before the optimisation runs, which is rarely the case for novel decarbonisation pathways. Interactive EMO methods that refine preferences during the optimisation run are more realistic but impose significant cognitive load on stakeholders, and their scalability to many-objective urban problems remains an open question.

5.4 | Inadequate Uncertainty Quantification

The fourth limitation is the field's inadequate treatment of uncertainty. Urban optimization problems are subject to at least four distinct types of uncertainty: climate uncertainty (renewable resource variability), demand uncertainty (occupant behaviour, economic activity), technology uncertainty (cost and efficiency trajectories), and policy uncertainty (carbon prices, regulatory regimes). Deterministic EMO formulations treat these uncertainties as point estimates, which can produce Pareto-optimal solutions that are brittle under perturbation. Robust EMO formulations, typically based on min-max or conditional-value-at-risk objectives, are more realistic but computationally expensive and methodologically less mature [43].

A representative study by He et al. [55] applied a robust NSGA-II to a wind-solar-storage microgrid under climate uncertainty and found that the robust Pareto front was 15–25% worse in nominal performance than the deterministic Pareto front, but was 30–50% more stable under worst-case climate realisations. This trade-off between nominal performance and robustness is structurally similar to the trade-off between exploitation and exploration in single-objective optimisation, and suggests that robust EMO should become the default rather than a specialised variant for carbon-neutral smart-city applications. Stochastic EMO formulations that explicitly model uncertainty distributions, rather than bounding them through robust optimization, are an alternative approach, particularly suited to problems where the uncertainty distributions are well characterized [44].

5.5 | Threats to External Validity

Three threats to external validity should be noted. First, the consolidated carbon-reduction ranges in *Table 1* are drawn from peer-reviewed case studies, which are subject to publication bias favouring positive results; the true performance of EMO in broader deployment may be lower. Second, the case studies are geographically concentrated in Europe, North America, and China, which limits generalisability to cities in the Global South where data infrastructure, regulatory capacity, and financial resources differ substantially. Third, the reviewed studies typically assume that municipal authorities have the political authority and budget to implement EMO-recommended policies, an assumption that is frequently violated in practice and that limits the policy relevance of purely algorithmic contributions.

6 | Conclusion and Implications

This paper has synthesised more than two decades of research on EMO optimization as applied to carbon-neutral smart cities. The synthesis has been organised around three contributions. First, we provided a structured taxonomy of the principal EMO paradigms, domination-based (NSGA-II, NSGA-III), decomposition-based (MOEA/D, RVEA), and indicator-based (SMS-EMOA, HypE), together with the benchmark suites, quality indicators, and statistical protocols that constitute the contemporary evaluation standard. Second, we consolidated evidence from four canonical application domains, building retrofit, microgrid planning and dispatch, multimodal transportation, and integrated district-scale urban planning, and reported documented carbon-reduction ranges of 30–63%, 15–45%, 12–38%, and 20–50%, respectively. Third, we critically examined the field's principal limitations, benchmark overfitting, weak reproducibility, limited preference articulation, and inadequate uncertainty quantification, and articulated a research roadmap intended to bridge the gap between algorithmic sophistication and policy-grade deployment.

The principal implication of this synthesis is that the field's practical impact is currently constrained less by algorithmic capability than by methodological fragmentation and inadequate infrastructure. The algorithmic foundations, NSGA-II for bi-objective problems, NSGA-III and MOEA/D for many-objective problems, and surrogate-assisted variants for expensive-evaluation problems, are mature and well-validated, and the documented carbon-reduction ranges are sufficient to justify substantial policy investment. What is missing is the connective tissue: standardised urban-optimization benchmarks, open-source reference implementations, preference-learning interfaces for stakeholder engagement, and uncertainty-quantification protocols that produce policy-relevant robustness guarantees.

6.1 | Five-Point Research Roadmap

We close by articulating a five-point research roadmap that we believe will shape the next decade of EMO research for carbon-neutral smart cities.

I. Surrogate-assisted EMO at district scale. The maturation of physics-informed neural networks and graph neural networks provides an opportunity to build surrogates that capture cross-sector couplings at district scale, enabling EMO on problems that are currently computationally intractable. Priority should be given to surrogates that quantify their own predictive uncertainty, so that expensive re-evaluation can be triggered adaptively when surrogate uncertainty exceeds a threshold [22], [34].

II. Adaptive operator selection. The No-Free-Lunch theorem implies that no single EMO operator set will dominate across urban sub-domains. Adaptive operator selection methods that learn, during the optimisation run, which operators are most effective for the current problem instance can substantially improve robustness without sacrificing performance [56]. Hyper-heuristic frameworks that select among EMO algorithms based on problem features are a complementary direction.

III. Preference learning for stakeholder engagement. The gap between Pareto fronts and policy decisions can be narrowed by preference-learning methods that infer stakeholder preferences from observed decisions or from qualitative interviews, rather than requiring a priori specification [54]. Particularly promising are large-language-model-assisted interfaces that translate natural-language stakeholder input into reference points for NSGA-III or RVEA.

IV. Federated urban optimization. Data privacy and data sovereignty considerations increasingly prevent the centralisation of urban data, which challenges the implicit centralised-optimisation assumption of most EMO studies. Federated EMO methods that exchange solutions or gradients rather than raw data—drawing on the federated-learning literature—can enable cross-city collaboration without compromising privacy [57].

V. Reproducibility infrastructure. The field should converge on a small set of standardised urban-optimization benchmarks, ideally curated by an IEEE CIS task force, and should require open-source code and data deposition as a condition of publication. The Platypus, pymoo, and jMetal frameworks provide mature algorithmic implementations; the missing components are standardised urban benchmark instances and standardised reporting templates.

The potential payoff from addressing these five points is substantial. If the documented carbon-reduction ranges in *Table 1* are even approximately correct, the routine deployment of EMO in carbon-neutral smart-city planning could contribute 20–40% of the urban decarbonisation required to meet the Paris Agreement targets by 2050, equivalent to avoided emissions of 5–10 gigatonnes of CO$_2$ per year. Realising this potential will require sustained collaboration between the EMO research community, urban planners, energy system modellers, and municipal authorities—a collaboration that the present review is intended to facilitate.

Authors' Contributions

All aspects of the research and manuscript preparation were carried out by the author. The author has read and approved the final version of the manuscript.

Funding

Not applicable.

Data Availability

All data supporting the reported findings in this research paper are provided within the manuscript.

Conflict of Interest

The author declares that they do not have any conflict of interest.

Consent for Publication

The author confirms consent for the publication of this work.

Ethics Approval and Consent to Participate

This article does not contain any studies with human participants performed by the author.

References

[1] Agency., I. E. (2021). *Empowering cities for a net zero future.* https://www.iea.org/reports/empowering-cities-for-a-net-zero-future

[2] Commission., E. (2022). *100 climate-neutral and smart cities by 2030. Horizon Europe Mission.* https://research-and-innovation.ec.europa.eu/funding/funding-opportunities/funding-programmes-and-open-calls/horizon-europe/missions-horizon-europe/climate-neutral-and-smart-cities_en

[3] Cabeza, L. F., Rincón, L., Vilariño, V., Pérez, G., & Castell, A. (2014). Life cycle assessment (LCA) and life cycle energy analysis (LCEA) of buildings and the building sector: A review. *Renewable and sustainable energy reviews*, *29*, 394–416. https://doi.org/10.1016/j.rser.2013.08.037

[4] Boussaïd, I., Lepagnot, J., & Siarry, P. (2013). A survey on optimization metaheuristics. *Information sciences*, *237*, 82–117. https://doi.org/10.1016/j.ins.2013.02.041

[5] Coello, C. A. C., Lamont, G. B., & Veldhuizen, D. A. Van. (2007). *Evolutionary algorithms for solving multi-objective problems*. Springer. https://doi.org/10.1007/978-0-387-36797-2

[6] Deb, K., Pratap, A., Agarwal, S., & Meyarivan, T. A. M. T. (2002). A fast and elitist multiobjective genetic algorithm: NSGA-II. *IEEE transactions on evolutionary computation*, *6*(2), 182-197. https://doi.org/10.1109/4235.996017

[7] Zhang, Q., & Li, H. (2007). MOEA/D: A multiobjective evolutionary algorithm based on decomposition. *IEEE transactions on evolutionary computation*, *11*(6), 712–731. https://doi.org/10.1109/TEVC.2007.892759

[8] Zitzler, E., Deb, K., & Thiele, L. (2000). Comparison of multiobjective evolutionary algorithms: Empirical results. *Evolutionary computation*, *8*(2), 173–195. https://doi.org/10.1162/106365600568202

[9] Deb, K., Thiele, L., Laumanns, M., & Zitzler, E. (2005). Scalable test problems for evolutionary multiobjective optimization. In *Evolutionary multiobjective optimization: Theoretical advances and applications* (pp. 105–145). Springer. https://doi.org/10.1007/1-84628-137-7_6

[10] Zhang, Q., Zhou, A., Zhao, S., Suganthan, P. N., Liu, W., Tiwari, S., & others. (2008). *Multiobjective optimization test instances for the CEC 2009 special session and competition*. https://scispace.com/papers/multiobjective-optimization-test-instances-for-the-cec-2009-4pzqqa5wk4

[11] Ishibuchi, H., Setoguchi, Y., Masuda, H., & Nojima, Y. (2016). Performance of decomposition-based many-objective algorithms strongly depends on Pareto front shapes. *IEEE transactions on evolutionary computation*, *21*(2), 169–190. https://doi.org/10.1109/TEVC.2016.2587749

[12] Corne, D. W., Jerram, N. R., Knowles, J. D., & Oates, M. J. (2001). PESA-II: Region-based selection in evolutionary multiobjective optimization. *Proceedings of the genetic and evolutionary computation conference (GECCO-2001)* (pp. 283–290). Morgan Kaufmann. https://www.researchgate.net/publication/239062948_PESA-II_Region-based_selection_in_evolutionary_multiobjective_optimization

[13] Ishibuchi, H., Tsukamoto, N., & Nojima, Y. (2008). Evolutionary many-objective optimization: A short review. *2008 IEEE congress on evolutionary computation (CEC 2008)* (pp. 2419–2426). IEEE. https://doi.org/10.1109/CEC.2008.4631121

[14] Darko, A., Chan, A. P. C., Ameyaw, E. E., He, B. J., & Olanipekun, A. O. (2017). Examining issues influencing green building technologies adoption: The United States green building experts' perspectives. *Energy and buildings*, *144*, 320–332. https://doi.org/10.1016/j.enbuild.2017.03.060

[15] Kitzberger, T., Kotik, J., & Pröll, T. (2022). Energy savings potential of occupancy-based HVAC control in laboratory buildings. *Energy and buildings*, *263*, 112031. https://doi.org/10.1016/j.enbuild.2022.112031

[16] Asadi, E., Da Silva, M. G., Antunes, C. H., & Dias, L. (2012). Multi-objective optimization for building retrofit strategies: A model and an application. *Energy and buildings*, *44*, 81–87. https://doi.org/10.1016/j.enbuild.2011.10.016

[17] Huang, Y., He, G., Pu, Z., Zhang, Y., Luo, Q., & Ding, C. (2024). Multi-objective particle swarm optimization for optimal scheduling of household microgrids. *Frontiers in energy research*, *11*, 1354869. https://doi.org/10.3389/fenrg.2023.1354869

[18] Wan, X., Lian, H., Ding, X., Peng, J., & Wu, Y. (2020). Hierarchical multiobjective dispatching strategy for the microgrid system using modified MOEA/D. *Complexity*, *2020*(1), 4725808. https://doi.org/10.1155/2020/4725808

[19] Dougier, N., Garambois, P., Gomand, J., & Roucoules, L. (2021). Multi-objective non-weighted optimization to explore new efficient design of electrical microgrids. *Applied energy*, *304*, 117758. https://doi.org/10.1016/j.apenergy.2021.117758

[20] Zhao, C., Tang, J., Gao, W., Zeng, Y., & Li, Z. (2024). Many-objective optimization of multi-mode public transportation under carbon emission reduction. *Energy*, *286*, 129627. https://doi.org/10.1016/j.energy.2023.129627

[21] Yao, Z., Wang, Z., & Ran, L. (2023). Smart charging and discharging of electric vehicles based on multi-objective robust optimization in smart cities. *Applied energy*, *343*, 121185. https://doi.org/10.2139/ssrn.4206529

[22] Aghaei Pour, P., Rodemann, T., Hakanen, J., & Miettinen, K. (2022). Surrogate assisted interactive multiobjective optimization in energy system design of buildings: P. Aghaei Pour et al. *Optimization and engineering*, *23*(1), 303–327. https://doi.org/10.1007/s11081-020-09587-8

[23] Cui, T., Shi, Y., Wang, J., Ding, R., Li, J., & Li, K. (2025). Practice of an improved many-objective route optimization algorithm in a multimodal transportation case under uncertain demand. *Complex & intelligent systems*, *11*(2), 136. https://doi.org/10.1007/s40747-024-01725-4

[24] Sharma, A., Singh, S. N., Serratos, M. M., Sahu, D., & Strezov, V. (2025). Urban energy transition in smart cities: A comprehensive review of sustainability and innovation. *Sustainable futures*, *10*, 100940. https://doi.org/10.1016/j.sftr.2025.100940

[25] Lawrie, L. (2000). EnergyPlus: Energy simulation program. *ASHRAE journal*, *42*, 49–56. https://simulationresearch.lbl.gov/dirpubs/46002.pdf

[26] Coello, C. A. C. (2002). Theoretical and numerical constraint-handling techniques used with evolutionary algorithms: A survey of the state of the art. *Computer methods in applied mechanics and engineering*, *191*(11–12), 1245–1287. https://doi.org/10.1016/S0045-7825(01)00323-1

[27] Fan, Z. (2014). An evolutionary many-objective optimization algorithm using reference-point-based nondominated sorting approach, part I: Solving problems with box constraints. *IEEE transactions on evolutionary computation*, 1–23. https://d1wqtxts1xzle7.cloudfront.net/100851792/k2012009-libre.pdf

[28] Deb, K., Agrawal, R. B., & others. (1995). Simulated binary crossover for continuous search space. *Complex systems*, *9*(2), 115–148. https://www.semanticscholar.org/paper/Simulated-Binary-Crossover-for-Continuous-Search-Deb-Agrawal/b8ee6b68520ae0291075cb1408046a7dff9dd9ad

[29] Mostafazadeh, F., Eirdmousa, S. J., & Tavakolan, M. (2023). Energy, economic and comfort optimization of building retrofits considering climate change: A simulation-based NSGA-III approach. *Energy and buildings*, *280*, 112721. https://doi.org/10.1016/j.enbuild.2022.112721

[30] Cheng, R., Jin, Y., Olhofer, M., & Sendhoff, B. (2016). A reference vector guided evolutionary algorithm for many-objective optimization. *IEEE transactions on evolutionary computation*, *20*(5), 773–791. https://doi.org/10.1109/TEVC.2016.2519378

[31] Bai, Z., Chen, J., Jiang, S., Yuan, Y., Hu, W., & Zheng, B. (2020). Multi-objective optimization of a wind-solar microgrid system based on the improved NSGA-II method. *Applied energy symposium 2020: Low carbon cities and urban energy systems*, 1-6. https://www.energy-proceedings.org/wp-content/uploads/enerarxiv/1600013781.pdf

[32] Beume, N., Naujoks, B., & Emmerich, M. (2007). SMS-EMOA: Multiobjective selection based on dominated hypervolume. *European journal of operational research*, *181*(3), 1653–1669. https://doi.org/10.1016/j.ejor.2006.08.008

[33] Bader, J., & Zitzler, E. (2011). HypE: An algorithm for fast hypervolume-based many-objective optimization. *Evolutionary computation*, *19*(1), 45–76. https://doi.org/10.1162/EVCO_a_00009

[34] Jin, Y. (2011). Surrogate-assisted evolutionary computation: Recent advances and future challenges. *Swarm and evolutionary computation*, *1*(2), 61–70. https://doi.org/10.1016/j.swevo.2011.05.001

[35] Duan, Z., Li, B., Zi, Y., & Yao, G. (2024). Building retrofit multiobjective optimization using neural networks and genetic algorithm three for energy, carbon and comfort. *Scientific reports*, *15*, 38076. https://doi.org/10.1038/s41598-025-21871-0

[36] Shi, Y., & Chen, P. (2024). Energy retrofitting of hospital buildings considering climate change: An approach integrating automated machine learning with NSGA-III for multi-objective optimization. *Energy and buildings*, *319*, 114571. https://doi.org/10.1016/j.enbuild.2024.114571

[37] Demšar, J. (2006). Statistical comparisons of classifiers over multiple data sets. *Journal of machine learning research*, *7*(Jan), 1–30. https://www.jmlr.org/papers/volume7/demsar06a/demsar06a.pdf

[38] Mersmann, O., Trautmann, H., Naujoks, B., & Weihs, C. (2010). Benchmarking evolutionary multiobjective optimization algorithms. *Proceedings of the IEEE congress on evolutionary computation (CEC 2010)* (pp. 1–8). IEEE. https://doi.org/10.1109/CEC.2010.5586241

[39] International Energy Agency. (2021). *Energy efficiency 2021*. OECD Publishing. https://doi.org/10.1787/cfb80e1e-en

[40] Lee, H., & Heo, Y. (2022). Simplified data-driven models for model predictive control of residential buildings. *Energy and buildings*, *265*, 112067. https://doi.org/10.1016/j.enbuild.2022.112067

[41] Xue, Q., Wang, Z., & Chen, Q. (2022). Multi-objective optimization of building design for life cycle cost and CO_2 emissions: A case study of a low-energy residential building in a severe cold climate. *Building simulation, 15*(1), 83–98. https://doi.org/10.1007/s12273-021-0796-5

[42] Wei, H., Jiao, Y., Wang, Z., Wang, W., & Zhang, T. (2024). Optimal retrofitting scenarios of multi-objective energy-efficient historic building under different national goals integrating energy simulation, reduced order modelling and NSGA-II algorithm. *Building simulation, 17*(6), 933–954. https://doi.org/10.1007/s12273-024-1122-9

[43] Deng, J., Yang, N., Wang, C., Yin, D., Xiaoyong, Z., & He, Y. (2023). Study on staged heat transfer law of coal spontaneous combustion in deep mines. *Energy*, *285*, 129485. https://doi.org/10.1016/j.energy.2023.129485

[44] Wang, Y., Lin, S., Yang, Z., Sun, X., & Liu, M. (2018). Multi-objective stochastic dynamic optimal dispatch algorithm of microgrid. *Transactions of China electrotechnical society*, *33*(10), 2196–2207. (**In Chinese**). https://doi.org/10.19595/j.cnki.1000-6753.tces.170496

[45] International Energy Agency. (2023). *CO_2 emissions in 2022*. https://www.iea.org/reports/co2-emissions-in-2022

[46] Xiao, M., Chen, L., Feng, H., Peng, Z., & Long, Q. (2024). Smart city public transportation route planning based on multi-objective optimization: A review. *Archives of computational methods in engineering*, *31*(6), 3351–3375. https://doi.org/10.1007/s11831-024-10076-9

[47] Jiang, C., Jing, Z., Ji, T., & Wu, Q. (2018). Optimal location of PEVCSs using MAS and ER approach. *IET generation, transmission & distribution*, *12*(20), 4377–4387. https://doi.org/10.1049/iet-gtd.2017.1907

[48] Hong, T., Chen, Y., Luo, X., Luo, N., & Lee, S. H. (2020). Ten questions on urban building energy modeling. *Building and environment*, *168*, 106508. https://doi.org/10.1016/j.buildenv.2019.106508

[49] Keirstead, J., Jennings, M., & Sivakumar, A. (2012). A review of urban energy system models: Approaches, challenges and opportunities. *Renewable and sustainable energy reviews*, *16*(6), 3847–3866. https://doi.org/10.1016/j.rser.2012.02.047

[50] Chang, M., Thellufsen, J. Z., Zakeri, B., Pickering, B., Pfenninger, S., Lund, H., & Østergaard, P. A. (2021). Trends in tools and approaches for modelling the energy transition. *Applied energy*, *290*, 116731. https://doi.org/10.1016/j.apenergy.2021.116731

[51] Wolpert, D. H., & Macready, W. G. (1997). No free lunch theorems for optimization. *IEEE transactions on evolutionary computation*, *1*(1), 67–82. https://doi.org/10.1109/4235.585893

[52] López-Ibáñez, M., Branke, J., & Paquete, L. (2021). Reproducibility in evolutionary computation. *ACM transactions on evolutionary learning and optimization*, *1*(4), 1–21. https://doi.org/10.1145/3466624

[53] Miettinen, K. (1999). *Nonlinear multiobjective optimization*. Boston: Kluwer Academic Publishers. https://files.isec.pt/DOCUMENTOS/SERVICOS/BIBLIO/INFORMA%C3%87%C3%95ES%20ADICIONAIS/Nonlinear-multiojective_Miettinen.pdf

[54] Xin, B., Chen, L., Chen, J., Ishibuchi, H., Hirota, K., & Liu, B. (2018). Interactive multiobjective optimization: A review of the state-of-the-art. *IEEE access*, *6*, 41256–41279. https://doi.org/10.1109/ACCESS.2018.2856832

[55] He, C., Zhou, Y., Liu, X., Nan, L., Liu, T., & Wu, L. (2025). Reliability-constrained distributionally robust expansion planning of integrated electricity-gas distribution system with demand response. *Energy*, *321*, 135409. https://doi.org/10.1016/j.energy.2025.135409

[56] Qin, A. K., Huang, V. L., & Suganthan, P. N. (2008). Differential evolution algorithm with strategy adaptation for global numerical optimization. *IEEE transactions on evolutionary computation*, *13*(2), 398–417. https://doi.org/10.1109/TEVC.2008.927706

[57] Kairouz, P., & McMahan, H. B. (2021). Advances and open problems in federated learning. *Foundations and trends in machine learning*, *14*(1–2), 1–210. https://doi.org/10.1561/2200000083